Effects of Diffusional Processes on Crystal Etching: Kinematic Theory Extended to Two Dimensions

Simon P. Garcia, Hailing Bao, and Melissa A. Hines*

Department of Chemistry, Cornell University, Ithaca, New York 14853

Received: September 24, 2003; In Final Form: February 18, 2004

The effects of diffusional processes on etching of crystalline materials are investigated using a model that combines an atomistic, kinetic Monte Carlo simulation with a step-density dependent model of diffusional effects. Diffusion may be driven by processes such as etchant depletion, product buildup, or reaction exothermicity. In effect, this model extends traditional kinematic theory (KT), a one-dimensional continuum model, to two dimensions. The case of relatively isotropic step flow etching with locally accelerating diffusional effects is examined in detail. When the effects of diffusion are included, the etching surface spontaneously develops step bunches separated by relatively step-free areas. Since diffusional processes accelerate etching, the step bunches travel faster than individual etching steps. The steady state size of the bunches is determined by the competition between step incorporation and step detachment. Both of these observations are in agreement with the original KT. In contrast, the characteristic concave bunch profile predicted by one-dimensional KT is not reproduced in two dimensions. Instead, the bunches have a relatively flat profile that is in agreement with recent experiments. The implications of this observation on experimental measurements are discussed.

1. Introduction

During etching or growth, crystalline materials often develop steplike features that are visible by eye or under an optical microscope. Although these features resemble atomic steps, they are much larger. Hence, they have been given the name "macrosteps". The production of macrosteps is not just an intellectual curiosity, as etching and growth are important industrial processes. For example, aqueous solutions of KOH are often used in the production of silicon microelectromechanical systems (MEMS).[1] These solutions produce macrosteps on some orientations of silicon. Similarly, macrostep formation on KDP (potassium dihydrogen phosphate) crystals is detrimental to the production of high quality nonlinear optical crystals.[2]

A widely invoked mechanism for the production of macrosteps in solution processes is often referred to as kinematic theory (KT) and was first put forth essentially simultaneously by Frank,[3] who described growth, and by Cabrera and Vermilyea,[4] who described etching. KT is based on the formation of *kinematic waves*, a mathematical construct developed by Lighthill and Whitham[5] to model river flow. This model is well-accepted and well-entrenched; it is quoted in essentially every monograph on etching (or growth). KT makes two very important simplifications—simplifications whose effect has not been examined in detail. First, KT is inherently one-dimensional. The atomic steps on an etching (or growing) crystal are treated as points on a line, not lines on a surface. Second, the profile of the etching (or growing) crystal is treated continuously; the discrete nature of atomic steps is not considered.

In this study, we remove both of these simplifications and consider the effects of diffusional processes on the evolution of the surface morphology. Diffusional effects may be induced by a variety of chemical processes, including etchant depletion, reactant buildup, and reaction exothermicity. We will show that although some of the predictions of KT carry over to two dimensions, there are important differences. In particular, one of the most fundamental predictions of KT—the production of step trains with a concave or convex shape—is not apparent in the two-dimensional, discrete theory. Nevertheless, features resembling kinematic waves are still apparent in the two-dimensional model.

The ultimate goal of these simulations is not, however, the reexamination of a 50-year-old model; it is the simulation of experimental data. For example, Figure 1 shows a scanning tunneling microscopy (STM) image of a miscut Si(111) surface after etching in an aqueous KOH solution.[6] Pronounced macrostep formation is readily apparent. As shown by the cross-sectional image (and detailed statistical studies), the etching-induced macrosteps are neither convex nor concave; in this respect, they do not resemble the macrosteps predicted by KT. Furthermore, the macrosteps have complicated lateral behavior. Individual steps sometimes cross between one macrostep and another, and individual macrosteps can merge and split. The complexity of these morphologies cannot be explained by traditional KT.

For simplicity, we only consider etching in this study. In principle, growth is the reverse of etching, so the major conclusions of this work are expected to hold for growth from solution, albeit with some changes in sign. Similarly, our model is based on the structure of the Si(111) surface; however, the major conclusions of this work should be applicable to *any* crystalline lattice.

Before introducing our model, we provide a brief overview of KT. More detailed expositions can be found in the literature.[7,8]

1.1. Kinematic Theory (KT). In kinematic theory, etching is only allowed at step sites, and the profile of the etching surface is modeled as a one-dimensional continuum. The etch rate (or velocity) of an individual step, v_{step}, is assumed to be a function of only the local step density, ρ_{step}. Mathematically, $v_{step} = f(\rho_{step})$. If the steps etch independently (i.e., there are no step-step interactions), all steps will move with the same velocity,

10.1021/jp036856i CCC: $27.50
Published on Web 04/15/2004

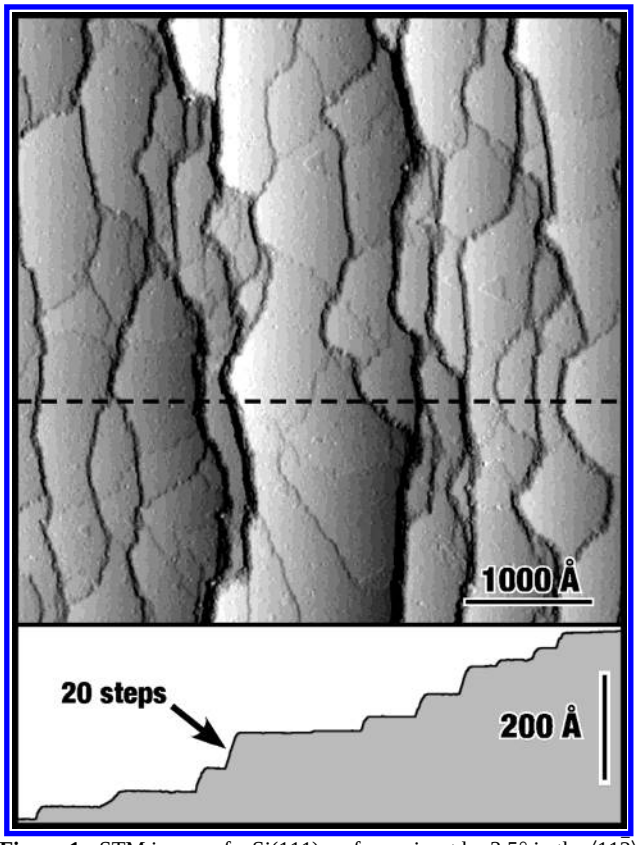

Figure 1. STM image of a Si(111) surface miscut by 3.5° in the ⟨112⟩ direction after etching for 5 min in an unstirred, room temperature, 50% (w/v) aqueous KOH solution. Although pronounced macrostep formation is visible, there are also many "crossing steps" connecting the macrosteps. A cross-sectional slice is indicated by the dashed line and displayed in the lower panel. No consistent preference for concavity or convexity is observed.

independent of the local step density and miscut. Under these conditions, KT predicts stable etching; no macrosteps will form.

The situation is very different if the step velocity is step-density dependent. For example, consider the case where etching is so rapid that the etchant becomes somewhat depleted in the vicinity of the surface. The depletion will be greatest above rapidly etching areas of the surface, which correspond to regions of high step density. This depletion will lead to the development of step bunches (macrosteps) in a manner analogous to the development of traffic jams on a crowded highway. When a random fluctuation brings two steps close to one another, enhanced depletion of the etchant causes the pair of steps to move more slowly. This slowed motion allows the next step in the train to catch up to the pair, creating an even more slowly traveling trio. This process continues, and a self-propagating step bunch is formed. Mathematically, this scenario occurs whenever $\partial v_{step}/\partial \rho_{step} < 0$. According to kinematic theory, any function that satisfies this general form will lead to the formation of *convex step bunches* with a discontinuity at the bottom of the bunch, as shown in Figure 2a.

A second type of kinematic wave is also possible. For example, a strongly exothermic etching reaction will locally heat the etchant (and surface.) This local heating will lead to a local acceleration of the etch rate, which will be most severe in regions of high step density. In this case, $\partial v_{step}/\partial \rho_{step} > 0$. This situation is also unstable to step bunching, and KT predicts the formation of *concave step bunches* with a discontinuity at the top of each bunch as shown in Figure 2b.

Although most descriptions of KT concentrate on the shape of the step bunches, it is important to realize that the step

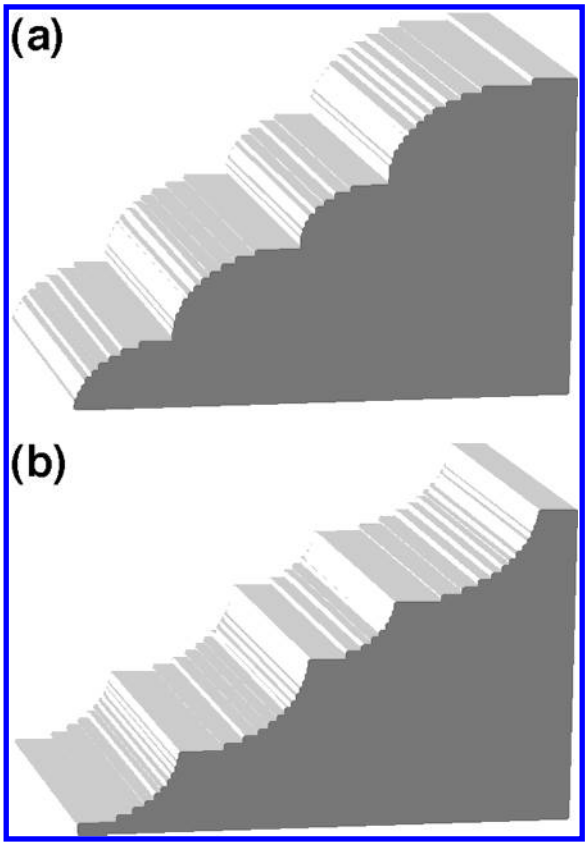

Figure 2. Schematic illustration of the bunches predicted by KT. (Because KT is a one-dimensional theory, only the surface profile is predicted.) (a) Convex bunches are formed when $\partial v_{step}/\partial \rho_{step} < 0$, whereas (b) concave bunches form when $\partial v_{step}/\partial \rho_{step} > 0$.

bunches predicted by KT are long-lived, self-propagating, *dynamic features* on the etching surface. Importantly, *the step bunches predicted by KT do not travel at the same velocity as the etching steps.* Convex step bunches, which are formed when $\partial v_{step}/\partial \rho_{step} < 0$, travel more slowly than the average step and are thus termed *negative bunches*. Conversely, concave step bunches travel faster than the average step and are termed *positive bunches.* In this respect, the propagation of kinematic waves resembles the propagation of shock waves (e.g., Cherenkov radiation), where the group velocity of the shock wave is different from the velocity of the component waves.

In summary, KT predicts the formation of kinetic instabilities, step bunches, during etching in any system in which the etch rate of individual steps is *step-density dependent.* These bunches are dynamic features of defined concavity or convexity that travel with a rate different from that of the etching steps.

1.2. General Description of New Two-Dimensional Model. The goal of this investigation is to examine the general effects that diffusional processes in the etchant have on the anisotropic etching of crystalline materials. In this study, we are more interested in obtaining qualitative insights into the evolution of surface morphology than in realistically modeling all of the microscopic processes that occur in a particular etching system. In effect, we are extending the original KT to the case of two-dimensional surfaces composed of discrete atoms while retaining the central postulate of KT, namely that the etch rate of a step is solely a function of the local step density.

Our model is based on an atomistic kinetic Monte Carlo (KMC) model of anisotropic Si(111) etching[9] that is capable of accurately reproducing the experimentally observed surface morphologies produced by well-stirred etchants (i.e., systems where diffusional processes are unimportant).[10,11] The original

KMC model is based on three postulates. First, the etch rate of a site on the surface is determined only by the structure of that site. For example, all kink sites are assumed to etch with the same rate, k_{kink}^{KMC}, whereas all terrace sites etch with a different rate, k_{terr}^{KMC}. In the model, seven different types of surface sites are defined:[12] a kink site, a terrace site, two types of stable step sites (corresponding to those produced by miscutting the surface in the $\langle 11\bar{2}\rangle$ and $\langle \bar{1}\bar{1}2\rangle$ directions), and three more esoteric species. Second, the model is based on the solid-on-solid approximation, so undercutting is disallowed. Finally, redeposition of silicon atoms from solution and diffusion of silicon atoms across the surface are explicitly forbidden. Under the conditions appropriate to aqueous silicon etching, both of these approximations are excellent. More details are given in previous publications.[9,12]

In the model presented here, we assume that the etch rate of a specific site, k_{site}, is determined by two parameters: the etch rate of that site under well-stirred conditions, k_{site}^{KMC}, and a modifying parameter that is a function of the local step density, $D(\rho_{step})$. This parameter represents the effect of any diffusional processes. Mathematically,

$$k_{site} = D(\rho_{step})k_{site}^{KMC} \quad (1)$$

The modifying parameter D describes the net effect of processes that change the local concentration or local temperature of the etchant. Importantly, D is a function of surface position (because it is dependent on local step density), but it is independent of the type of step site. In general, D will be greater than 1 if the diffusional process accelerates etching locally (e.g., if the reaction exothermicity leads to a local temperature increase), whereas it will be less than 1 if the diffusional process leads to local deceleration (e.g., if etching locally depletes the etchant). If the diffusional process has no effect on etching, $D = 1$.

In moving from the one-dimensional, continuous KT to the new two-dimensional, discrete model, the definition of local step density needs to be carefully considered. In KT, the step density has a unique definition—it is the slope of the surface profile at a given point. Three uncertainties arise in moving to two dimensions. First, two-dimensional steps have lateral extent. In general, the etching steps will not be perfectly straight; they will meander. Because of this, the step density is not constant across the entire length of a step. Instead, the density must be defined for every point along the step. Second, the local density of a set of discrete objects, such as steps, is not uniquely defined. Over what length scale should the density be averaged? Third, a discrete atomistic model must include terrace sites as well as step sites. If these sites are allowed to etch, as they do in reality, how should the step density above the terrace be defined? If diffusional processes affect etching, should not terrace sites near a step see a higher step density than those in the middle of a terrace?

In defining the function ρ_{step}, we draw inspiration from diffusion itself. Figure 3a shows the morphology of an etching surface at one particular point in time. If the reaction exothermicity generates a local temperature rise in the etchant which is modeled as a constant heat source, the etching of the site marked by an arrow in Figure 3a would lead to a temperature rise of some characteristic extent. This rise is sketched for two different characteristic distances in Figure 3b,c. If the same amount of heat were simultaneously released from every atom on the etching steps, the thermal profiles in Figure 3d,e, which are simple sums over individual sources centered on each etching atom, would instead result.

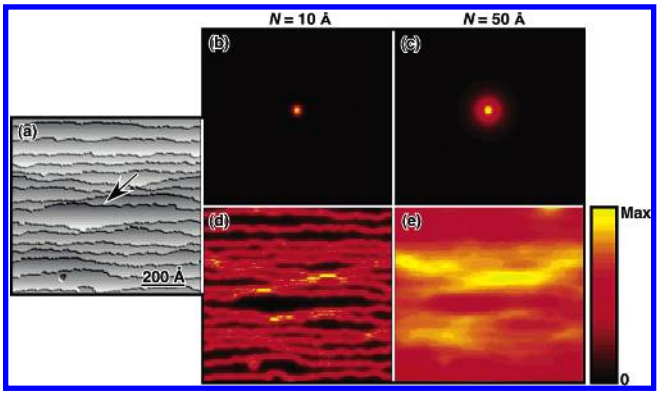

Figure 3. Illustration of the step density function (see text). (a) The morphology of an etching surface. (b), (c) Normalized temperature rise above that surface induced by a constant heat source located at one point (indicated by arrow) on the etching surface. (The parameter N is described in section 2.1.) (d), (e) Normalized temperature rise that would be induced by heat sources located at every step site on the etching surface.

For the case of diffusional processes, the functions represented by Figure 3d,e are both reasonable definitions of "local step density" in two dimensions in that they satisfy the preceding criteria. Obviously, the two cases differ in their averaging distance (i.e., their definition of "local"); this averaging distance must therefore be specified as a parameter in our model. In both cases, the density is highest where steps are in close proximity. This can be caused either by the close approach of neighboring steps, by protrusions in a single step, or by some combination of the two. Importantly, the step density is uniquely defined at every point on the etching surface, and the step density at terrace sites is defined in a reasonable manner.

In adopting this definition of step density, we do not mean to imply that the actual thermal gradient (or etchant concentration gradient) above the surface has this exact profile. Clearly, sites on the surface do not etch synchronously, and the steps do move with time. This functional form is, however, a convenient and computationally tractable means to realistically extend the definition of step density to two dimensions.

In the following, we first describe the computational model and then discuss means of parametrizing the simulated surface morphologies. We then present an overview of the types of morphological changes that can be produced during isotropic step flow etching in the presence of diffusional processes that accelerate etching. The effects of etchant anisotropy and decelerating diffusional processes will be discussed in forthcoming manuscripts.

2. Computational Details

In the original formulation of KT, the functional form of the dependence of the step etch rate on step density was not specified; only the sign of the first derivative of this function was considered. As a result, the original model made no predictions about the size of step bunches or the magnitude of the concavity/convexity. In this study, we investigated two different functional forms of step density dependence.

This model is an extension of a two-dimensional KMC simulation of Si(111) etching that has been described in detail previously.[9] In the following, we describe only the extensions to this model. In section 2.1, we describe the calculation of the local step density function, which was introduced in Figure 3d,e. In section 2.2, we discuss the effect of the local step density on the etch rate—in other words, the calculation of D in eq 1. In section 2.3, we discuss an efficient algorithm for the new KMC

TABLE 1: Characteristic Length Scale Corresponding to Different Values of the Length Scale Paramater, *N*[a]

N	extent
5 Å	24 Å
10 Å	46 Å
20 Å	92 Å
40 Å	184 Å

[a] See text for details.

simulation. Finally, in section 2.4, we briefly describe the methods used to parametrize the etch morphologies obtained in later sections.

2.1. Local Step Density Function. During the calculation, the local step density is represented by a two-dimensional matrix that has the same spatial extent as the etching surface. Like the simulation, the step density matrix has toroidal boundaries to simulate an infinite surface. The calculation of the step density matrix for an arbitrary surface morphology proceeds as follows. In our simulation, every nonterrace surface atom is defined to be a step site. As a consequence, there are two types of steps: vicinal steps and steps surrounding etch pits. Starting from an initially zeroed step density matrix, one is added to the matrix at the (x, y) position of every defect (i.e., nonterrace) site. In effect, this process outlines the step edges in the step density matrix. Once the locations of all step sites are recorded in the step density matrix, the matrix is convoluted with a normalized kernel,[13] which represents the effect of diffusion.

Two different (normalized) kernels were investigated. The first kernel was a Gaussian,

$$G = \frac{1}{\pi n^2} e^{-r^2/n^2} \tag{2}$$

where r is the distance from the center of the kernel, whereas the second was a decaying exponential,

$$K = \frac{1}{2\pi N^2} e^{-r/N} \tag{3}$$

A Gaussian form is appropriate for the diffusion from an instantaneous pulsed source at some later time, whereas the exponential form is appropriate for steady state diffusion resulting from a continuous, stationary source. The constants n and N control the length over which the step density is averaged. Although these two kernels have significantly different functional forms, the morphologies produced by the kernels were *nearly identical*, as judged by eye and by statistical parametrizations (vide infra). No consistent difference was observed in the size, shape, concavity or propagation of the macrosteps produced by the two kernels or in the morphology or number of the crossing steps. (Of course, identical morphologies did not result for identical values of n and N, as these parameters represent slightly different length scales.) Because of this marked similarity, we only present simulations based on the second (exponential) kernel in the following.

The only difference between the step densities depicted in Figure 3d,e, which were generated with the exponential kernel, is the value of N; Figure 3d was calculated with a smaller value of N than Figure 3e. Table 1 gives the characteristic length scale for a number of values of N. (Here, the characteristic distance is defined to be the distance, measured perpendicular to the step edge, over which a single infinite step would have a step density greater than 10% of its maximum value.)

2.2. Effect of Step Density on Local Etch Rate: Acceleration vs Deceleration. As in the original formulation of KT, the local step density may either accelerate or decelerate etching. Diffusional processes that locally accelerate etching include reaction exothermicity and the buildup of products in autocatalytic reactions. Diffusional processes that decelerate etching include reagent depletion and product buildup in non-autocatalytic reactions. In eq 1, the net effect of all diffusional processes is represented by $D(\rho_{step})$. In general, $D > 1$ when diffusional processes accelerate etching, whereas $D < 1$ when they decelerate etching.

Broadly speaking, we have found that the morphological effects of diffusional processes are determined largely by whether the processes have a net accelerating or net decelerating effect on etching. In contrast, the functional form of D on ρ_{step} has only a minor morphological effect as long as one criterion is met: D cannot go to zero. In a solid-on-solid model, where undercutting is explicitly forbidden, an unetchable point will lead to the production of an ever-growing hillock. As such, the morphology will not reach steady state.

In our model, we used one of two functional forms for D depending on the nature of the diffusional process being simulated. For the case of accelerating etchants, we used a simple linear form:

$$\text{Acceleration:} \qquad D = 1 + a\rho_{step} \tag{4}$$

Alternatively, decelerating etchants used a similar linear form that was truncated to keep D finite and positive:

$$\text{Deceleration:} \qquad D = \max\begin{bmatrix} 1 - a\rho_{step} \\ 0.1 \end{bmatrix} \tag{5}$$

Both of these forms have a single adjustable parameter, a, which controls the "strength" of the diffusional effects. For example, a relatively large value of a would correspond to high values of etchant depletion (in deceleration mode) or reaction exothermicity (in acceleration mode), whereas small values would correspond to little depletion or a small exothermicity. The exact value of the cutoff in deceleration mode (here, 0.1) had relatively little effect on the morphological results.

In this manuscript, we concentrate on the development of the model and the effects of diffusion-induced acceleration (eq 4) on relatively isotropic step-flow etchants. In future manuscripts, we will explore the effects of decelerating etchants and etchant anisotropy.

2.3. Etching Algorithm. Anisotropic etchants often attack different sites with radically different etch rates. For example, aqueous NH_4F solutions attack Si(111) kink sites 10^7 times more rapidly than terrace sites![14] For this reason, anisotropic etchants produce surface morphologies with very anisotropic site distributions. The NH_4F etchant produces atomically flat Si(111) surfaces in which the nearly unreactive terrace sites can outnumber the highly reactive kink sites by many orders of magnitude. These dramatic disparities in site density and reactivity place stringent demands on the simulation.

In the standard approach to Monte Carlo simulation, a random number is chosen to determine whether a randomly chosen site on the surface will be etched. In the case of anisotropic etching, this approach would be extremely inefficient, as huge quantities of random numbers would have to be generated (on average) for every successful etching event. To avoid this problem, we use the n-fold method introduced by Bortz and co-workers.[15] The n-fold method turns the problem around and uses a random number to determine *which site* will be the next to etch. At the expense of some added bookkeeping, each random number leads

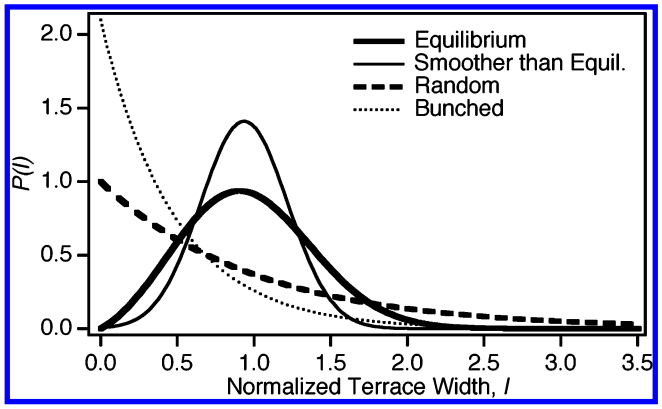

Figure 4. Effects of morphology on the terrace width distribution, $P(l)$. See text for details.

to an etching event. A detailed description of our implementation of the *n*-fold method is given in ref 9.

The situation considered here is more complex, because the probability of etching a specific site is determined both by its type (e.g., kink, terrace) and by the value of D at that point. The *n*-fold method cannot be efficiently implemented in this system, so we use a hybrid method of calculation. Using the *n*-fold method, we first chose a random number to determine which site would be the next to etch in the *absence of diffusional effects*. We then chose a second random number to decide whether to accept the etching of that site on the basis of the value of D at that site.

2.4. Parametrization of the Etch Morphology and Definition of Bunching. One of the thorniest issues in the study of surface morphology is parametrization. The problem is simple—how can a complex, two-dimensional morphology produced by a stochastic process be best reduced to a few numbers to enable comparison with other morphologies? For example, how should one measure the extent of step bunching? Or determine whether the steps are bunched? This topic has received a great deal of attention over the past decade, and many parametrizations have been developed (e.g., fractal analysis, autocorrelation functions, local widths, spectral power). A number of these methods are described in detail in ref 16. Despite this effort, no one parametrization has emerged as the clear leader for all morphologies. Different morphologies apparently require different parametrizations. In the following, we use two primary parametrization methods: terrace width distributions (TWDs) and height difference functions.

Terrace width distributions are most useful in the parametrization of nearly ideal, vicinal surface morphologies. Generally speaking, there are two interesting limiting distributions, as illustrated in Figure 4. Equilibrium vicinal surfaces (e.g., well-annealed surfaces) will have a near-Gaussian normalized TWD[17−19] of the (approximate[20]) form

$$P(l) = 1.5(1 - e^{-l/0.85})e^{-(l-0.75)^2/0.5} \quad (6)$$

where L is the terrace width, and $l = L/\langle L\rangle$. In this distribution, the most probable terrace width is $\sim 0.91\langle L\rangle$. The simplest type of step-flow etching—a two-dimensional terrace-step-kink model with no terrace etching—leads to a nearly identical TWD, even though the etching surface is clearly not in equilibrium.[21] Interestingly, when a finite rate of terrace etching (and hence a low density of etch pits) is included in the model, a much smoother surface, with a narrower TWD, results.[21] In all of these nearly flat morphologies, the most interesting parameter is the width of the distribution. The second type of limiting distribution is a random distribution, which leads to an exponential TWD

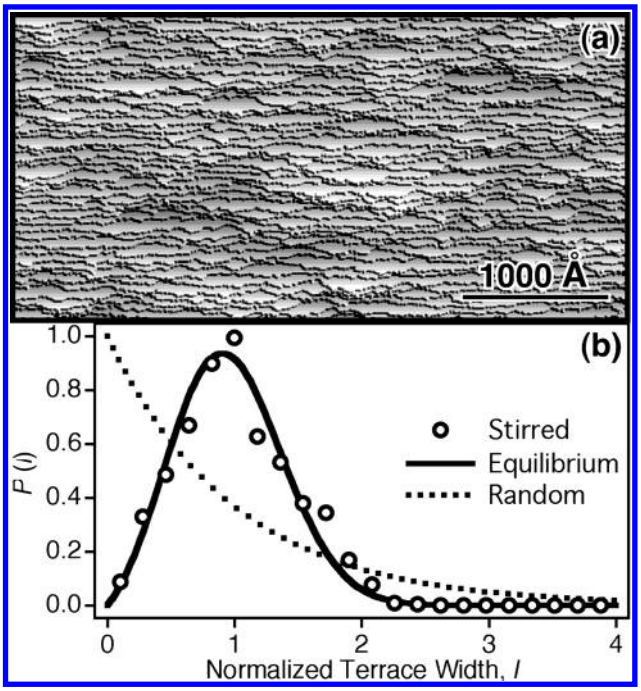

Figure 5. In the absence of diffusion-induced inhomogeneities, anisotropic step etching leads to relatively smooth surfaces, as shown by both the (a) steady state morphology and (b) terrace width distribution.

of the form

$$P(l) = e^{-l} \quad (7)$$

Interestingly, some types of complicated step etching lead to this distribution as well.[12]

In the absence of a generally accepted mathematical definition of bunching, we adopt an empirical definition. Since step bunching leads to a proliferation of short terraces, any morphology that leads to a TWD that is more skewed toward zero than a random (exponential) distribution is said to be "bunched."

Although a useful indicator of bunching, TWDs contain no information on the characteristic size and spacing of step bunches. For this, an analysis that reflects spatial correlations is needed. In the following, we use the height difference function (or height-height correlation function), H, which is defined to be

$$H(\vec{a}) = \langle (z(\vec{r}) - z(\vec{r} + \vec{a}))^2 \rangle^{1/2} \quad (8)$$

where $z(\vec{r})$ is the height of the surface at point $\vec{r}$ (measured with respect to the best-fit plane) and the brackets denote an average over all points on the surface. In the limit of large $\vec{a}$, H is the root-mean-square (RMS) roughness of the surface, whereas $H(0)$ is identically zero.

3. Results

To illustrate the general results of the new two-dimensional model, we concentrate in this manuscript on the case of a relatively isotropic step flow etchant. The etchant is assumed to attack all step sites with approximately the same etch rate; however, terrace sites are unreactive. Because of this, no etch pits develop. In the absence of any diffusional effects, this etchant produces a relatively flat, steady state morphology characterized by meandering steps, as shown in Figure 5a. Because the etching steps are not allowed to undercut one another, there is an effective repulsion between the etching steps.

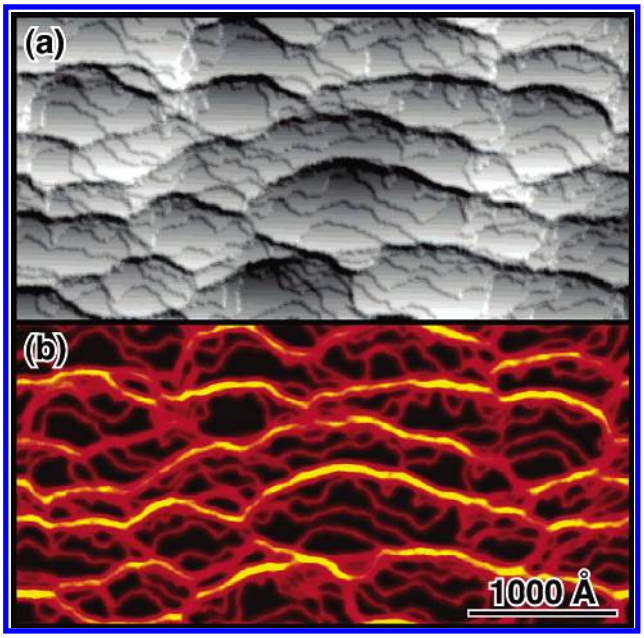

Figure 6. Diffusion-induced inhomogeneities lead to the development of step bunches. (a) Steady state morphology obtained with $N = 20$ Å and $a = 20$, and (b) the corresponding step density function. The color scale is the same as in Figure 3.

As a result, the steady state morphology displays a near-equilibrium TWD, as shown by Figure 5b and discussed in detail in ref 21. (The deviations from this limiting distribution appear to be due to the discrete nature of terrace widths in an atomistic simulation.) It should be noted that this near-equilibrium TWD would not be seen in a one-dimensional model, such as KT, as there is no dynamical repulsion in one-dimensional models. Instead, an exponential TWD would result.

All of the simulations reported here were performed on Si(111) surfaces miscut by 3.5° toward the $\langle 11\bar{2} \rangle$ direction. The average step spacing was 50 Å, and 42 vicinal steps were included in each simulation. The simulations included approximately 1.5 million surface atoms.

In the following, diffusion is assumed to have an *accelerating effect* on etching. This type of kinetics might be applicable to a strongly exothermic reaction. Regions of high step density would be highly reactive and thus somewhat warmer than regions of low step density. The functional form of D is therefore given by eq 4.

3.1. Development of Step Bunches. When the effects of diffusion are included, the etch morphology undergoes a dramatic transformation. The etching surface develops step bunches separated by individual steps, as seen in Figure 6a. The corresponding step density function, ρ_{step}, is shown in Figure 6b. This transformation is relatively insensitive to the chosen parameters (i.e., the interaction strength, a, and the length scale parameter, N).

After an initial induction period, the surface does not continue to roughen during etching. Instead, the surface reaches a steady state morphology. Although the details of this morphology evolve continuously, the average size and structure of the macrosteps do not. The existence of a steady state morphology is reflected in a number of different statistical parameters. For example, Figure 7 shows the temporal evolution of the root-mean-square roughness, R, of the etching surface, which is given by

$$R = \sqrt{\langle z^2 \rangle} \tag{9}$$

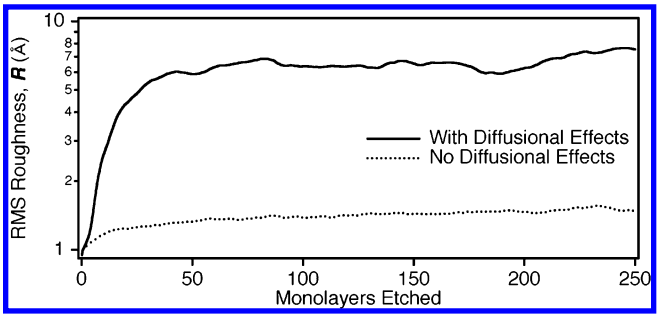

Figure 7. Evolution of the RMS roughness as a function of number of monolayers etched from an initially flat surface. The solid line represents $N = 20$ Å and $a = 20$ (see Figure 6), and the dotted line represents a well-stirred etchant (e.g., Figure 5).

For comparison, the roughness of the surface in the absence of diffusional effects (e.g., Figure 5) is shown by a dotted line. In both cases, the simulation started from a perfect vicinal surface with negligible roughness. The surface roughness underwent an initial rapid increase as the etch morphology developed, but after this induction time, the roughness remained relatively constant.

Step bunches develop during etching, but do these bunches correspond to the kinematic waves in KT? One of the hallmarks of kinematic waves is their velocity. In the case of accelerating kinetics, where $\partial v_{step}/\rho_{step} > 0$, a kinematic wave should travel *faster* than the etching steps. This is indeed observed, as shown by the sequence of morphologies in Figure 8, which were extracted from Movie S1 in the online Supporting Information.[22] In these images, a single, arbitrary terrace is shown in color, whereas a single step bunch is marked by arrows. At the beginning of the sequence [i.e., after 130 monolayers (ML) have been etched from the surface], the highlighted terrace is part of the bunch indicated by the blue arrows. Initially, both the bunch and the terrace move upward at approximately the same velocity; however, the terrace begins to detach from the center of the bunch at 136 ML. Once the terrace detaches from the bunch, its velocity slows dramatically. As a result, it is rapidly overtaken by the next bunch in the train. This process can be seen at 142 ML where the previously detached center region of the highlighted terrace begins to incorporate into the trailing bunch. Many more examples of this behavior can be observed in Movie S1. Since the step bunches are dynamic features that move *faster* than the etching steps, we conclude that they are indeed the analogue of kinematic waves in KT.

If the bunches move faster than individual steps, why are there any isolated steps in the steady state morphology? Why do not the bunches grow without bound, overtaking and incorporating all slower species, such as isolated steps and smaller bunches? The answer to this conundrum can also be seen in Figure 8. At the beginning of the sequence, the highlighted terrace is completely incorporated in the step bunch. After 136 ML of etching, random fluctuations cause a few regions of the step to lag behind the bunch. These regions immediately begin to etch more slowly, "dragging" neighboring regions back. By 142 ML, a significant portion of the step has detached from the original bunch. This process of detachment progresses in succeeding images, while the next bunch in the train begins to overtake the slowed step. At 142 ML, the initially detached region makes contact with the next bunch and begins the process of incorporation. As a result of this process, the steady state bunch size (i.e., the average number of steps per bunch) is determined by the competition between step incorporation and step detachment.

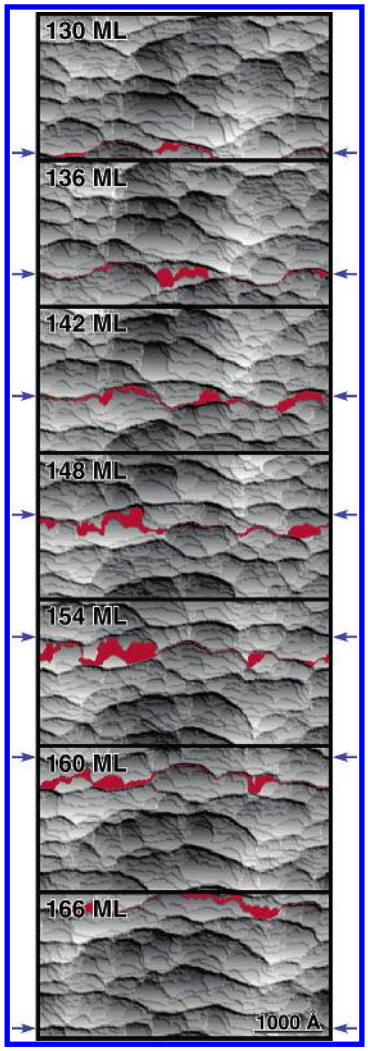

Figure 8. Temporal sequence of etch morphologies ($N = 20$ Å, $a = 20$) illustrating the different velocities of isolated steps and step bunches. A single arbitrary terrace has been highlighted in this sequence. The arrows indicate the progress of a single bunch.

Before examining the shape of the bunches in detail, we next examine the effects of the two adjustable parameters in the model—the interaction strength, a, and the length scale parameter, N.

3.2. Effect of the Interaction Strength Parameter. The interaction strength parameter, a, determines the sensitivity of the etch rate to the step density. For example, in the case where reaction exothermicity drives step bunching, increasing the exothermicity of the reaction would lead to an increase in a.

The effects of the interaction strength parameter are illustrated by the steady state morphologies (left panels) and height difference functions (right panels) in Figure 9. The solid black lines superimposed on the height difference functions represent the 65% of maximum contours, which roughly correspond to the characteristic distances between macrosteps. In a well-stirred solution where diffusional effects are negligible (i.e., $a = 0$), step meandering leads to relatively small regions of perfection. As a result, the 65% contour is relatively small. In contrast, step bunching leads to significantly larger step-free areas and correspondingly larger 65% contours.

Interestingly, the height difference functions show that increasing interaction strength primarily affects the size of the step-free areas in the direction perpendicular to the step edges; it has little effect on the lateral extent of these regions. This effect can be understood from the etch morphologies. When

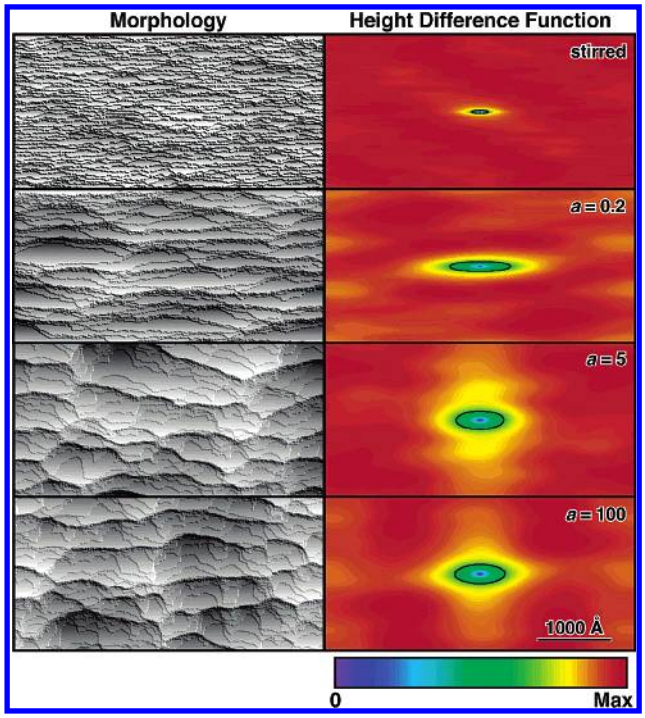

Figure 9. Effect of a on the steady state morphologies and normalized height difference functions. The solid line in the height difference function represents the 65% contour. For all simulations, $N = 20$ Å.

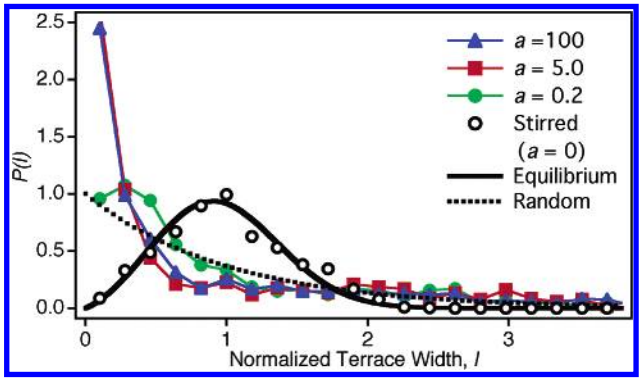

Figure 10. Terrace width distributions corresponding to the steady state morphologies in Figure 9.

the interaction strength is low, the etching steps meander but remain relatively straight. As the interaction strength is increased, the steps become more strongly attracted to the bunches, and thus more difficult to detach. As a result, partially detached steps often develop segments that are nearly perpendicular to the bunch direction. This behavior is most clearly seen in the $a = 100$ morphology.

By eye, increasing interaction strength is also correlated with increasing bunch size; however, this effect appears to saturate at high values of a. This trend is confirmed by changes in the TWDs with increasing interaction strength, as shown in Figure 10. In the absence of diffusional effects, the terrace width distribution resembles that of a surface in equilibrium. This observation is consistent with previous research[21] and indicative of a weak dynamic repulsion between the etching steps. (Dynamic repulsion is not seen in one dimension; KT would predict an exponential TWD.) When diffusional effects are included, the TWDs become very strongly skewed toward zero terrace width—much more skewed than a random distribution—which is consistent with step bunching. From the trends in the TWDs, we conclude that increasing interaction strength leads to a small increase in the degree of step bunching.

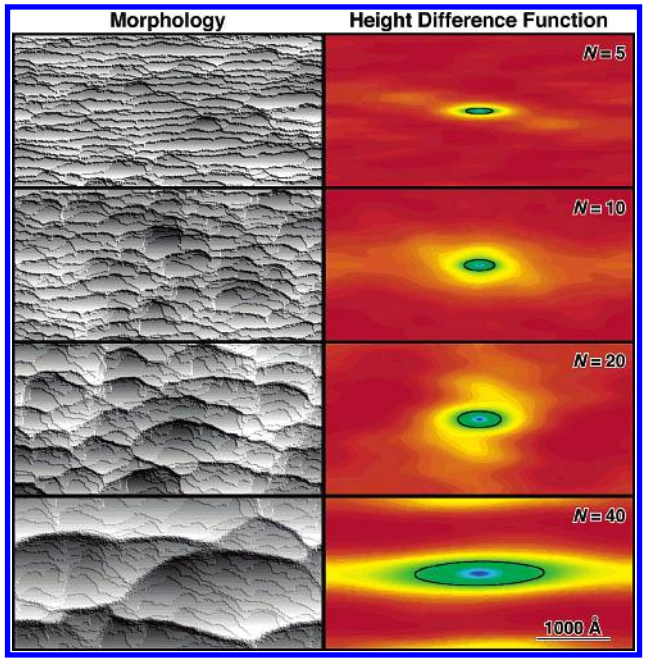

Figure 11. Effect of N on the steady state morphologies and normalized height difference functions. The solid line in the height difference function represents the 65% contour. For all simulations, $a = 20$. The height difference function scale is the same as in Figure 9.

3.3. Effect of the Length Scale Parameter. In this model, the length scale parameter N defines the distance over which the step density is averaged, as indicated by Table 1 and Figure 3. (As noted previously, this parameter has no analogue in the original one-dimensional model, which was defined in terms of the differential quantity, $\partial v_{step}/\partial \rho_{step}$.) In physical terms, the length scale parameter is determined by the relative rates of etching and diffusion. Rapid etching or slow diffusion would correspond to relatively small values of the length scale parameter, whereas slow etching or rapid diffusion would correspond to larger values.

This parameter has similar, but not identical, effects to those of the interaction strength parameter, as shown by the morphologies and height difference functions in Figure 11. Increasing the length scale parameter increases the amount of step bunching while also increasing the average distance between step bunches. As shown by the height difference functions, increasing the length scale parameter increases the average size of the step-free areas in both directions. Of course, this behavior cannot continue unbounded. In the limit where N approaches infinity, all of the inhomogeneities in the system will disappear, and the simulation must return to the "stirred" (i.e., $a = 0$) morphology. The $N = 5$ Å simulation, which has a characteristic averaging length of 24 Å or $\sim 1/2$ of the average step spacing, is worthy of note, as this simulation displays a marked preference for step doubling over multistep bunch formation. A qualitatively similar type of bunching was observed experimentally in the NH_4F(aq) etching of miscut Si(111) surfaces.[23]

Increased step bunching is also observed in the TWDs, as shown in Figure 12. As the length scale parameter is increased, the distributions become more skewed toward zero terrace width—an indication of increased bunching.

The length scale parameter and the interaction strength parameter have very different effects on the step morphology. Large values of the length scale parameter do not lead to the formation of the near vertical regions of step seen in Figure 9. Instead, increasing the length scale parameter leads to longer wavelength meandering of the step bunches. This difference is reflected in the shape of the 65% maximum contours on the height difference functions.

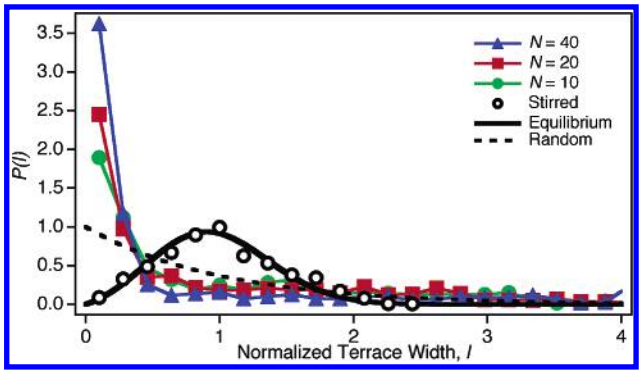

Figure 12. Terrace width distributions corresponding to the steady state morphologies in Figure 11.

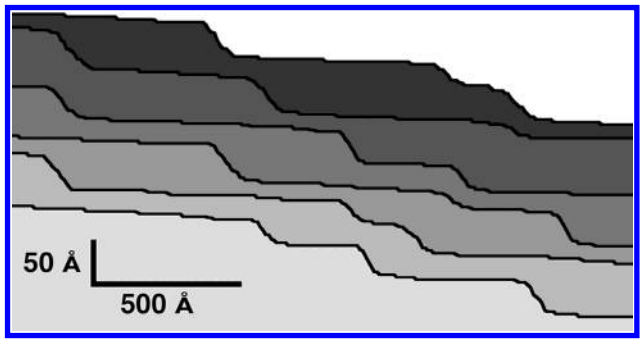

Figure 13. Six arbitrarily chosen cross-sections of bunched steady state surface morphologies ($N = 40$ Å, $a = 20$) illustrating the absence of defined concavity or convexity.

3.4. Step Bunch Profiles: Absence of Concavity. The most frequently mentioned prediction of one-dimensional kinematic theory is the formation of convex and concave step bunches. According to the one-dimensional theory, the accelerating kinetics studied here should produce concave step bunches. Interestingly, *we find no convincing evidence* of this behavior in two dimensions.

To illustrate this, Figure 13 shows six arbitrarily chosen profiles from the steady state morphologies of simulations displaying severe step bunching (i.e., $a = 20$, $N = 40$ Å). Most of the bunches have a relatively flat profile, and no consistent concavity or convexity is observed. According to the one-dimensional theory, concave step bunches should also display a discontinuity in the step profile at the uppermost point of each bunch. No evidence for this discontinuity is observed.

After examining many different morphologies produced under a wide variety of simulation parameters, we conclude that diffusional effects *do not* lead to a characteristic concavity of the bunch profile, at least within the confines of this model. The simulated profiles are, however, similar to those observed experimentally (e.g., Figure 1).

4. Discussion

4.1. Comparison with One-Dimensional Model. The predictions of the two-dimensional model of diffusion-enhanced etching presented here bear many similarities to those of the original one-dimensional model developed over 50 years ago. Nevertheless, there are also a number of important differences. In agreement with the original model, we find that step-flow etching with relatively isotropic kinetics is *unstable* to the formation of step bunches if regions of high step density etch faster than regions of low step density. This instability is

relatively insensitive to the choice of model parameters that describe the diffusional process. Like the old model, the new model also predicts the formation of features resembling kinematic waves—self-propagating, dynamic step bunches that, in this case, travel more quickly than individual etching steps.

Importantly, the two-dimensional model *does not reproduce* the bunch morphology predicted previously. The one-dimensional model predicts the formation of bunches with characteristic concavity or convexity. For the case of accelerating etchants studied here, concave step bunches with a discontinuity at the upper edge of the bunch are predicted by the old model. In contrast, the two-dimensional model produced relatively flat bunches with no consistent concavity or convexity.

These findings have important implications on experimental studies of macrostep formation. First and foremost, *the step bunch profile cannot be used as a reliable indicator of step-density dependent etch kinetics*. In particular, the absence of concavity is not necessarily associated with a step-density independent etch rate. We note, however, that the effects of reaction anisotropy (i.e., site-specificity) and decelerating kinetics on the step bunch profile remain to be examined in detail. Second, although the production of kinematic waves is easily detected from the temporal evolution of the etch morphology, we have been unable to identify a definitive *static* indicator of these dynamic features. As a result, a definitive identification of kinematic waves from static AFM or STM measurements may be problematic. Third, diffusional effects have a significant effect on the morphology of etched steps. Because of this, the reaction anisotropy cannot be extracted from the step morphology *unless* these diffusional effects are taken into consideration. As a result, the methods that we previously developed to quantify site-specific etch rates from morphological measurements[9] cannot and should not be applied to quiescent etchants. For these methods to be applicable, any mesoscale inhomogeneities in the etchant must be removed, perhaps through stirring or agitation.

In this work, we have also made no attempt to calculate or estimate the most appropriate values for the two parameters used in this model: the interaction parameter, a, and the length scale parameter, N. Since diffusion is relatively rapid in aqueous solutions, aqueous silicon etchants, such as KOH, may require larger values of N than those presented here. On the other hand, the macrosteps observed in the experimental image shown in Figure 1 are comparable in magnitude and separation to the largest macrosteps seen in Figure 11. We have also shown that the general conclusions we have drawn from this model are relatively independent of the simulation parameters. Extrapolating from our current results, we predict that larger values of N would lead to larger step bunches separated by larger distances; however, this trend should reverse after N increases above a maximal value, since our model must revert to the stirring (no acceleration) case when N approaches infinity.

4.2. Comparison with Other Bunching Mechanisms. The model presented here is not appropriate for all types of bunching instabilities. In particular, there is a class of asymmetric mechanisms for bunching that are linearly unstable. In these mechanisms, the instability is driven by an asymmetry in the etch rate with respect to the terrace in front of and behind a given step. This type of asymmetry was first studied by Bennema and Gilmer.[24]

In their analysis, the etch rate of a step was assumed to have the functional form

$$v_{\text{step}} = f_+(\lambda_+) + f_-(\lambda_-) \tag{10}$$

where λ_+ and λ_- are the widths, respectively, of the terraces in front of and behind the step. Bennema and Gilmer[24] showed that a small perturbation in an equidistant series of steps would grow exponentially if

$$\frac{\partial f_+}{\partial \lambda} > \frac{\partial f_-}{\partial \lambda} \tag{11}$$

In other words, the instability was attributed to the asymmetric dependence of the etch rate on the forward and backward terrace widths. This asymmetry led to spontaneous bunching.

A number of systems have been identified that display an asymmetry of this type. For example, step bunching during step-flow evaporation (i.e., etching) into a vapor can be induced by an Ehrlich−Schwoebel (ES) barrier.[24,25] When an atom detaches from a step edge, it can either detach onto the upstairs terrace or the downstairs terrace. In systems with an ES barrier, detachment onto the downstairs terrace (that is, the terrace behind the etching step) is energetically favored, and there is a net flux of atoms in the downstairs direction. Since the etching step's velocity will depend more strongly on the width of the terrace behind it, $f'_+(\lambda) < f'_-(\lambda)$. As a result, an ES barrier will lead to etching-induced step bunching.

In contrast, our model has a symmetric dependence on the forward and reverse terrace widths. According to the criterion identified by Bennema and Gilmer and expressed in eq 11, our model should be stable to the formation of macrosteps. This observation shows that an asymmetry is not necessary for macrostep formation.

Another commonly cited mechanism for step bunching, contamination from the etchant, has been described using models that are symmetric or asymmetric with respect to the forward and backward terrace widths. In the most comprehensive study, Kandel and Weeks argued that the chemistry in this system is inherently asymmetric and that the asymmetry plays an important role in inducing the step-bunching instability.[26,27] When an etching surface is subjected to a constant, isotropic flux of contaminants from the etchant, the probability of contaminating any specific site is constant in time. This does not imply that the density of contaminants on the surface is isotropic, though. As the surface etches, new, uncontaminated sites are continuously exposed to the etchant. Because of this, sites below an ascending step edge have a lower probability of contamination than sites that are farther away from the ascending step. If contaminated sites etch more slowly than uncontaminated sites (a reasonable assumption), the velocity of an etching step will depend on the width of the upstairs terrace (λ_+) but not on the width of the downstairs terrace (λ_-). In this situation, linear stability theory predicts that step bunching will result. Kandel and Weeks also performed two-dimensional Monte Carlo simulations of contamination-induced step bunching.[27] The morphologies predicted by their simulations bear some similarities to those presented here even though the two models differ in their forward/backward symmetry.

In his original work on KT, Frank also discussed the effect of impurity adsorption on crystal etching.[3] Although he clearly recognized the asymmetry discussed by Kandel and Weeks, he did not consider the effects of this asymmetry explicitly. Instead, he argued that steps bounded by wide terraces, which correspond to regions of low step density, would be more contaminated than those bounded by narrow terraces. This leads to a negative dependence of the etch rate on terrace width. As a result, he used KT to predict the formation of concave step bunches in contaminated etchants.

5. Conclusions

During etching, diffusional processes lead to the development of microscopic inhomogeneities in the near-surface region during etching. These inhomogeneities, which may be due to etchant depletion, product buildup, or reaction exothermicity, may cause a local acceleration or deceleration of etching. To simulate these processes, a model that combines an atomistic kinetic Monte Carlo simulation with a step-density dependent model of diffusional effects has been developed. In effect, this model extends the original kinematic theory model to two dimensions. This model has two adjustable parameters that control the length scale of the inhomogeneities as well as the strength (or coupling) between the etch rate and the diffusional inhomogeneities.

The case of relatively isotropic step flow etching in the presence of locally accelerating diffusional effects has been examined in detail. Under these conditions, diffusional inhomogeneities lead to the production of step bunches. The step bunches travel faster than isolated steps, in agreement with the predictions of the original KT. The bunches are dynamic structures whose steady state size is determined by the competition between step attachment and detachment. In these respects, the new two-dimensional model is in good agreement with the original one-dimensional KT.

In contrast, the characteristic concave bunch profiles predicted by one-dimensional KT are not apparent in two dimensions. Instead, the simulated bunches have a relatively flat profile. Because of this, the definitive identification of kinematic waves from static morphologies may prove to be problematic.

Acknowledgment. This material was supported in part by the NSF under Award No. CHE-0138026 and by the Center for Nanoscale Systems (NSF EEC-0117770). Acknowledgment is also made to the donors of the Petroleum Research Fund, administered by the American Chemical Society, for partial support of this research. This work made use of the Cornell Center for Materials Research Shared Experimental Facilities, supported through the NSF Materials Research Science and Engineering Centers program.

Supporting Information Available: A QuickTime movie showing the development of step bunches during the etching of an initially perfect vicinal Si(111) surface is available for download.[22] To illustrate the flow of steps, a single terrace is colored red. Because of the toroidal boundary conditions, steps that etch off the top of the simulation reappear at the bottom. This material is available free of charge via the Internet at http://pubs.acs.org.

References and Notes

(1) Elwenspoek, M.; Jansen, H. V. *Silicon Micromachining*; Cambridge University Press: Cambridge, U.K., 1998.
(2) Robey, H. F.; Potapenko, S. Y. *J. Cryst. Growth* **2000**, *213*, 355.
(3) Frank, F. C. On the Kinematic Theory of Crystal Growth and Dissolution Processes. In *Growth and Perfection of Crystals*; Doremus, R. H., Roberts, B. W., Turnbull, D., Eds.; Wiley: New York, 1958; p 411.
(4) Cabrera, N.; Vermilyea, D. A. The Growth of Crystals from Solution. In *Growth and Perfection of Crystals*; Doremus, R. H., Roberts, B. W., Turnbull, D., Eds.; Wiley: New York, 1958; p 393.
(5) Lighthill, M. J.; Whitham, G. B. *Proc. R. Soc.* **1955**, *229*, 281.
(6) Garcia, S. P.; Bao, H.; Hines, M. A. Unpublished results.
(7) Sangwal, K. *Etching of Crystals: Theory, Experiment and Application*; North-Holland: Amsterdam, 1987; Chapters 4 and 8.
(8) Heimann, R. B. Principles of Chemical Etching − The Art and Science of Etching Crystals. In *Silicon Chemical Etching*; Grabmaier, J., Ed.; Springer-Verlag: Berlin, 1982; Vol. 8, p 173.
(9) Flidr, J.; Huang, Y. C.; Newton, T. A.; Hines, M. A. *J. Chem. Phys.* **1998**, *108*, 5542.
(10) Newton, T. A.; Huang, Y. C.; Lepak, L. A.; Hines, M. A. *J. Chem. Phys.* **1999**, *111*, 9125.
(11) Garcia, S. P.; Bao, H.; Manimaran, M.; Hines, M. A. *J. Phys. Chem. B* **2002**, *106*, 8258.
(12) Flidr, J.; Huang, Y. C.; Hines, M. A. *J. Chem. Phys.* **1999**, *111*, 6970.
(13) For a discussion of convolution, see: Press, W. H.; Teukolsky, S. A.; Vetterling, W. T.; Flannery, B. P. *Numerical Recipes in C*, 2nd ed.; Cambridge: Cambridge, U.K., 1992; Chapter 12.
(14) Hines, M. A. *Int. Rev. Phys. Chem.* **2001**, *20*, 645.
(15) Bortz, A. B.; Kalos, M. H.; Lebowitz, J. L. *J. Comput. Phys.* **1975**, *17*, 11.
(16) Barabási, A.-L.; Stanley, H. E. *Fractal Concepts in Surface Growth*; University of Cambridge: Cambridge, U.K., 1995.
(17) Fisher, M. E.; Fisher, D. S. *Phys. Rev. B* **1982**, *25*, 3192.
(18) Joós, B.; Einstein, T. L.; Bartelt, N. C. *Phys. Rev. B* **1991**, *43*, 8153.
(19) Einstein, T. L.; Pierre-Louis, O. *Surf. Sci.* **1999**, *424*, L299.
(20) This is an empirical fit to the exact solution given in ref 18. For an alternate approximation, see ref 19.
(21) Huang, Y. C.; Flidr, J.; Newton, T. A.; Hines, M. A. *J. Chem. Phys.* **1998**, *109*, 5025.
(22) Movie S1 can also be viewed at http://www.chem.cornell.edu/mah11/StepFlowMoov.html.
(23) Huang, Y. C.; Flidr, J.; Newton, T. A.; Hines, M. A. *Phys. Rev. Lett.* **1998,** *80*, 4462.
(24) Bennema, P.; Gilmer, G. H. Kinetics of Crystal Growth. In *Crystal Growth: An Introduction*; Hartman, P., Ed.; North-Holland Publishing Co.: Amsterdam, 191.
(25) Sato, M.; Uwaha, M. *Surf. Sci.* **2001**, *493*, 494.
(26) Kandel, D.; Weeks, J. D. *Phys. Rev. B* **1994**, *49*, 5554.
(27) Kandel, D.; Weeks, J. D. *Phys. Rev. B* **1995**, *52*, 2154.